

Optimal sizing of a standalone renewable energy reverse osmosis desalination system using an ant system

Daming Xu

School of Mechanical Engineering
Xi'an University of Science and Technology
Xi'an, China
xu_daming@hotmail.com

Thomas L. Acker

Professor of Mechanical Engineering
Northern Arizona University
Flagstaff, Arizona, USA
tom.acker@nau.edu

Abstract—The purpose of this work was to find the optimal configuration for an off-grid, renewable energy reverse osmosis (RO) desalination system using an ant system (AS), where the objective was to find the lowest annualized cost of the renewable energy system. This nonlinear integer programming was transferred to finding the shortest route on the construction graph by artificial ants. A well on the Navajo Nation in Arizona, USA was selected as the candidate site and real-world data were used. The capacity of the RO system was 18.93 m³/d (5000 gal/d), requiring a constant power consumption of 3.95 kW. The results of the AS optimization showed that the optimal configuration with the smallest annualized cost of the renewable energy system was a hybrid wind/photovoltaic/battery system, although a diesel generator was a candidate. The cost of energy was 0.46 USD/ kWh and cost of water was 3.35 USD/m³, which was less than half of the 7.9 USD/m³ currently paid by residents that live in the area.

Keywords— brackish water desalination, reverse osmosis, renewable energy, optimal sizing, ant colony optimization

I. INTRODUCTION

Access to affordable, reliable electricity and clean drinking water remain as two of the greatest challenges facing society. In rural areas with brackish water where renewable energy resources exist, reverse osmosis (RO) desalination is a good choice for water desalination [1]. Finding optimal economic configurations of renewable energy (RE) powered desalination plants is a challenging task, especially in remote or arid areas.

The artificial intelligence-based techniques for optimal design of renewable energy hybrid power systems include genetic algorithm (GA), particle swarm optimization (PSO), evolutionary particle swarm optimization (EPSO) and ant colony optimization (ACO) etc. [2]. ACO is an optimization technique which was introduced in the early 1990's. Foraging behavior of real ant colonies was the starting point of ACO: natural ants are able to find shortest paths between anthill and

food by a particular type of reinforcement learning, with pheromone trails for information exchange. Dorigo, Maniezzo and Colorni have transferred this principle to ACO algorithms [3]. This behavior was exploited in artificial ant colonies for searching approximate solutions to discrete and continuous optimization problems [4]. The three most popular ACO algorithms are ant system (AS), ant colony system (ACS), and MAX-MIN ant system (MMAS) [5]. ACO has been used in problems that can be encoded as “best path” problems such as traveling salesman, routing in telecommunication networks, graph coloring, scheduling and clustering, as well as hybrid power optimization.

The Southwest Navajo Nation (SNN) is a rural area in northeastern Arizona, US, which has a large amount of accessible brackish groundwater with poor water quality. The SNN has about 12,000 residents, who haul potable water, averaging 0.38 m³ (100 gal) per capita of for household and livestock use. In transporting this water, residents drive an average of 48 km per day and costing 3 to 10 USD per 0.38 m³ of potable water [6]. The Navajo Nation, in consultation with the U.S. Bureau of Reclamation, has made the decision to develop a desalination system powered by renewable energy at Leupp Coconino County, Arizona (35.4313°N, 111.1123°W), where brine pumped water physical condition is 1,000 mg/L of dissolved minerals.

A fresh water production of 18.93 m³/d (5,000 gal/d) through RO was chosen at Leupp. The objective was to find the optimal, least cost, configuration for a renewable energy reverse osmosis desalination (REROD) system, which can be formulated as a nonlinear integer programming (NIP) problem. An ant system was used to solve the NIP problem.

II. PROBLEM FORMULATIONS

Figure 1 shows a schematic of the studied REROD system. The system consists of two main parts: an RE system and an RO

system. The electric power consumption of the RO system was assumed to be constant [7]. Thus, the focus of this study was the optimal sizing of the RE system instead of the entire REROD system.

The RE system was built upon an alternating current (AC) bus. The voltage and frequency stability depends upon one diesel generator (DG) and a cluster of bi-directional converters connected to a battery bank. The cluster of bi-directional converters is the central control unit, which dispatches the diesel power generation through a signal cable connection. The solar and wind power generation are connected to the AC bus via inverters, and the RO system gets its power supply from the AC bus.

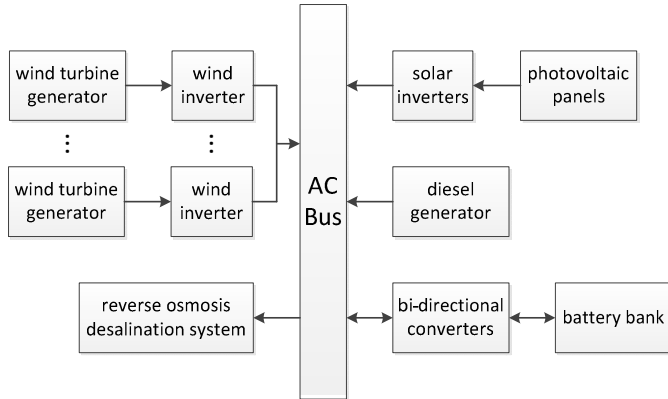


Fig. 1. Schematic of the REROD system.

The RE system may be composed of combinations of the following components: solar photovoltaic (PV) panels, wind turbine generators (WTGs), a diesel generator (DG), battery energy storage (batt) and power conditioning equipment such as solar inverters, wind inverters and bi-directional converters. To perform the simulation, it was necessary to build mathematical models of each RE system component and the load, which is the RO system power consumption. These models and the power system logistical models were described in the open access paper [8].

To supply the electrical load, the power resources are dispatched in the following order: 1) the WTGs and PV panels; 2) the batteries; and, 3) the DG [9][10], employing the micro-cycling dispatch strategy [11]. The DG starts when the battery state of charge (SOC) drops to a defined set point (SOC_{start}), and stops if the renewable energy production plus the battery bank can cover the load. Thus, the DG is dispatched to cover the load when there is insufficient energy produced by the wind and/or solar resources at the beginning of any time step t , and if the battery state of charge is insufficient, i.e. $SOC_t < SOC_{start}$ (in this modeling, SOC_{start} is 50%). In the following time step, if renewable energy plus the battery bank adequately covers the load and $SOC_t > SOC_{start}$, then the DG stops; otherwise, the DG keeps running. When the SOC_t is 100% and if there is excess renewable energy, the renewable power generation will be constrained.

When considering the composition of REROD, it is possible that a candidate RE system will not have a DG, batteries, or both. Thus when dispatching the batteries and/or DG in the energy

system, it is possible that during some hours of the year that the will be a loss of power supply (LPS). The loss of supply probability (LPSP) is then calculated by dividing the LPS by the total electrical energy load during the year. In such cases, the simulation sums the total energy deficit over the year. For any given candidate RE system, if the LPSP is above a predefined threshold, then the system configuration is discarded as an infeasible solution. For this simulation, the RO system is assumed to be running all the time, thus any RE system with an $LPSP > 0$ is discarded as infeasible.

III. COST MODELS

The annualized cost models [12][13] were employed to analyze both system and component costs. The annualized cost of a PV panel AC_{PV} is the sum of its annualized capital cost CC_{PV} and operation and maintenance cost OMC_{PV} .

$$AC_{PV} = CC_{PV} + OMC_{PV} \quad (1)$$

where

$$CC_{PV} = CRF \cdot C_{PV,a} \quad (2)$$

$$OMC_{PV} = \left(CRF \sum_{x=0}^{n-1} \frac{1}{(1+r)^x} \right) C_{PV,ma} \quad (3)$$

$$CRF = \frac{r(1+r)^n}{(1+r)^n - 1} \quad (4)$$

CRF is capital recovery factor. $C_{PV,a}$ and $C_{PV,ma}$ are acquisition cost of a PV panel and maintenance cost of a PV panel per year, respectively. r is discount rate and n is analysis period.

Annualized costs of WTGs, power conditioning equipment, RO equipment and the tank were calculated in the same way as explained for a PV panel. For a DG or a battery bank there could be replacements and fuel consumption, so the derivative formulas of above cost analysis method were used [12].

The annualized cost of the RE system AC_{sys_RE} is the sum of all the annualized costs of the components in the power system [12][13]. The cost of energy (COE) is expressed as [13]:

$$COE = \frac{AC_{sys, RE}}{E_{RO, year}} \quad (5)$$

where $E_{RO, year}$ is annual energy demand from the RO system. Following the definition of COE, the cost of water (COW) is defined below:

$$COW = \frac{AC_{sys, REROD}}{D_{WD} \times 365} \quad (6)$$

where

$$AC_{sys, REROD} = AC_{sys, RE} + AC_{sys, RO}$$

and D_{WD} is daily volumetric fresh water demand.

IV. OPTIMIZATION PROBLEM

The optimal sizing of the RE system was formulated as a single criteria integer programming as:

$$\left\{ \begin{array}{l} \min AC_{\text{sys, RE}} \\ \text{s.t.} \\ \text{LPSP} \leq \text{LPSP}_{\text{set}} \\ N_{\text{WTG}_y} = 0, 1, 2, \dots, 15, y=\text{I,II,III} \\ N_{\text{PV, para}} = 0, 1, 2, \dots, 60 \\ N_{\text{batt, para}} = 0, 1, 2, \dots, 60 \\ N_{\text{DG}} = 0, 1 \end{array} \right. \quad (7)$$

The objective was to minimize the annualized cost of the RE system $AC_{\text{sys,RE}}$. The LPSP was set as the constraint for feasible solutions, and is represented by the LPSP_{set} . The capacities of every type of WTG, PV panel sizes, battery capacities and DG sizes have a considerable influence on the power reliability and RE system annualized cost and can be optimized. All the decision variables were integer. The optimization is a NIP problem with the constraint calculated by simulation.

From a practical point of view, the amount of radiation received using PV panels with a fixed tilt angle equal to the latitude is only slightly less than that using a monthly adjusted tilt angle. The fixed tilt angle method was employed because it requires less-expensive equipment and less maintenance [14].

V. THE ANT SYSTEM

A construction graph of the AS was built according to the NIP problem in this research, shown in Figure 2. The construction graph contains the following components [2][3]:

(a) On the construction graph, except the start node, each node represents a decision variable. For a node, each incident arc represents an integer value assigned to the variable. A construction graph specifies a particular encoding of the solutions, which are feasible or infeasible, as ‘walks’. The objective function value of one walk is that of the solution the walk represents.

(b) Initially, m ants are placed on the start node (Node 0), from which they start their trips. An ant stochastically selects an arc with a transition probability (see Equation (8)) to get to the next node. If all ants get to the end node (Node N_{var}) this round of trip ends and this was called an iteration. The refusal strategy was introduced. In an iteration, if an ant’s walk represents an infeasible solution, the ant must start new trips until its walk represents a feasible solution. An application of the AS consists of many iterations.

(c) Transition probabilities are used to determine the movement of the ants. The probabilistic choice of an arc from node $i-1$ to node i is biased upon the pheromone trail $\tau_{i,j}(n_{\text{iter}})$ and heuristic information $\eta_{i,j}$, where i is node pointer, j is arc pointer and n_{iter} is iteration counter. Let heuristic information

$\eta_{i,j} = 1/(AC_i \cdot IV_{i,j})$, where AC_i is the annualized cost of the equipment related to node i and $IV_{i,j}$ is the integer value that node i arc j represents. For the AS, ant k currently located at node $i-1$ chooses arc j to go to node i with a probability

$$p_{i,j}^k(n_{\text{iter}}) = \frac{[\tau_{i,j}(n_{\text{iter}})]^\gamma [\eta_{i,j}]^\omega}{\sum_{s \in F_i} [\tau_{i,s}(n_{\text{iter}})]^\gamma [\eta_{i,s}]^\omega} \quad (8)$$

where γ and ω are two parameters representing the relative importance of the pheromone trail and the heuristic information. F_i is the range of integer value of node i .

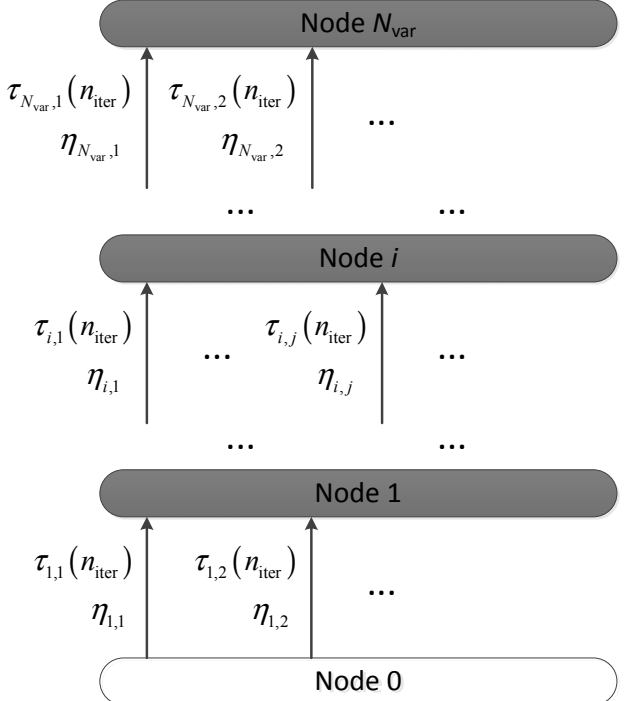


Fig. 2. Construction graph of the Ant system.

(d) $\tau_{i,j}$ as array of pheromone values, where $\tau_{i,j}$ is assigned to arc (i, j) on the construction graph. After all ants have completed trips in an iteration, the pheromone values are updated following this rule:

$$\tau_{i,j}(n_{\text{iter}} + 1) = \rho \tau_{i,j}(n_{\text{iter}}) + \sum_{k \in Fe(n_{\text{iter}})} \Delta \tau_{i,j}^k(n_{\text{iter}}) \quad (9)$$

where the parameter ρ (with $0 \leq \rho < 1$) is the trail persistence (thus, $1 - \rho$ models the evaporation), $\Delta \tau_{i,j}^k(n_{\text{iter}})$ is pheromone amount ant k puts on arc (i, j) given it has passed arc (i, j) as a feasible solution and $Fe(n_{\text{iter}})$ is the set of all the feasible ants passing arc (i, j) in iteration n_{iter} . Because of the refusal strategy, $Fe(n_{\text{iter}})$ is always the entire ant population. N_{iter} is the total number of iterations. The evaporation mechanism helps to avoid unlimited accumulation of the

pheromone trail. When an arc is not chosen by the ants, its associated pheromone trail decreases exponentially. This enables the algorithm to ‘forget’ bad choices over time. In the AS, $\Delta\tau_{i,j}^k(n_{\text{iter}})$ was defined as:

$$\Delta\tau_{i,j}^k(n_{\text{iter}}) = \begin{cases} 1/AC_{\text{sys,RE}}^k(n_{\text{iter}}) & \text{if arc}(i,j) \text{ belongs to the feasible} \\ & \text{walk by ant } k \text{ in iteration } n_{\text{iter}}, \\ 0 & \text{otherwise} \end{cases} \quad (10)$$

where $AC_{\text{sys,RE}}^k(n_{\text{iter}})$ is the annualized cost of the RE system obtained by the feasible walk of ant k in iteration n_{iter} . By Equation (8), the better the ant’s trip is, the more pheromone is received by the arcs in this trip.

VI. DATA

The third-version typical meteorological year data sets (TMY3s) contain hourly solar radiation data and meteorological data for a 1-year period [15]. The location of Winslow, Arizona at latitude 35.033°N and longitude 110.717°W, and elevation 1490m was chosen, which is nearest to Leupp among the locations in TMY3s. Global horizontal radiation, wind speed, diffuse horizontal radiation, extraterrestrial horizontal radiation and temperature in the TMY3s were employed, with the ground reflectance $\rho_G = 0.2$.

The technical specifications and economic data for each of the RE system components are shown in Table 2 of paper [8], along with the discount rate as 3% and project lifetime as 10 years. The rated power of the three types of WTGs were 1 kW, 2 kW and 3 kW.

VII. RESULTS AND DISCUSSION

The numbers of PV panels and batteries in series were determined as 3 and 24, respectively, in order to match the input voltage requirements of their respective inverters. On the construction graph, the node matrix [Node1, Node2, Node2, Node4, Node5, Node6] is defined as: [WTG_I, WTG_{II}, WTG_{III}, a series of PV panels, a series of batteries, DG], and then a solution is described as [N_{WTG_I} N_{WTG_II} N_{WTG_III} $N_{\text{PV, para}}$ $N_{\text{batt, para}}$ N_{DG}], where WTG_I is type I WTG and N_{WTG_I} is the number of WTG_I, WTG_{II} is type II WTG and N_{WTG_II} is the number of WTG_{II}, and so on. The fixed tilt angle was set as 35°. The simulation results for each walk of an ant include the annual fuel consumption, DG running time and battery bank Ah output. These outputs were used in the cost analysis. In this research, the settings for the AS are $m=200$, $N_{\text{iter}}=50$, $\gamma=1$, $\omega=5$, $\rho=0.8$, and for the REROD system simulation are $LPSP_{\text{set}}=0$, $SOC_{\text{start}}=0.5$ and project lifetime $n=10$ years.

Running the AS resulted in walk [0 3 0 24 30 0] having the lowest $AC_{\text{sys,RE}} = 15855$ USD/year and corresponding $AC_{\text{sys,REROD}} = 23139$ USD/year, and therefore being identified as the optimal solution. In words, this individual RE system was composed of three type II WTGs (2 kW), with 24 strings of PV panels, with 30 strings of batteries and the DG was not selected.

Figure 3 shows the monthly power generation of the optimal solution, in which solar energy accounts for the largest proportion. Figure 4 shows the monthly SOC of the battery bank for a TMY3 year of the optimal solution. Most of the time the SOC is above 0.8, which is in favor of battery lifetime, and consequently during the 10-year life of the system there was no battery bank replacement

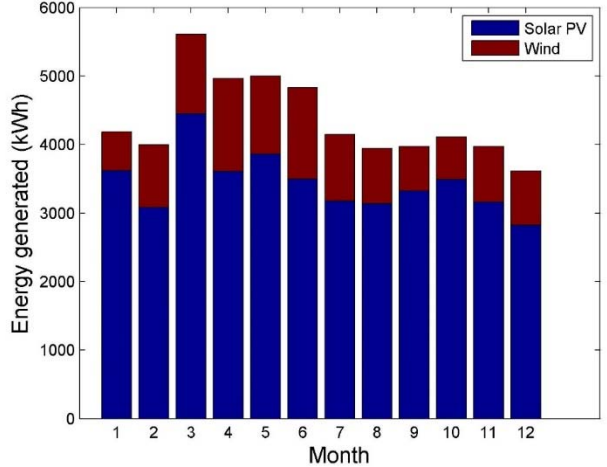


Fig. 3. Monthly power generation of the optimal solution [0 3 0 24 30 0].

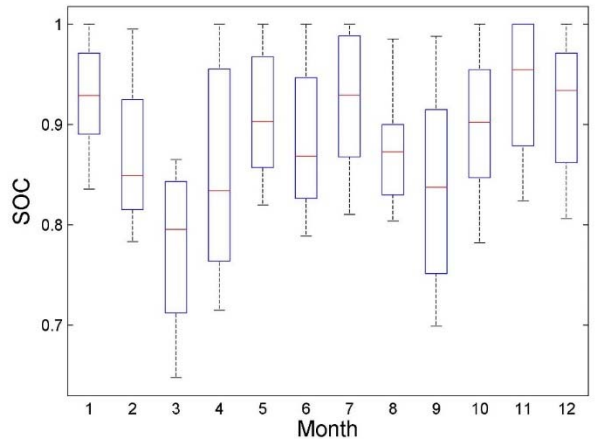


Fig. 4. Monthly SOC of the optimal solution [0 3 0 24 30 0].

If a DG was compulsorily included, the optimal solution was [0 4 0 13 25 1], with $AC_{\text{sys,RE}} = 16270$ USD/year and corresponding $AC_{\text{sys,REROD}} = 23554$ USD/year. Figure 5 shows the monthly power generation of the optimal solution, in which the DG almost shuts down from Mar. to Jun. and runs to complement the insufficient renewable energy in the fall and winter. Figure 6 shows the monthly SOC of the battery bank for a TMY3 year of the optimal solution. Most of the time the SOC is near 0.6, which does harm to battery lifetime but makes more renewable energy utilized. During the 10-year life of the system there was no battery bank replacement. If this kind of combination is used in real world, frequent equilibrium charging by the DG is a must for the sake of battery lifetime

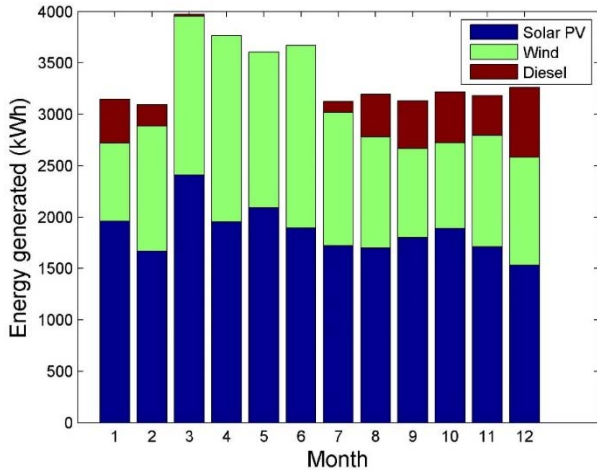


Fig. 5. Monthly power generation of the optimal solution [0 4 0 13 25 1].

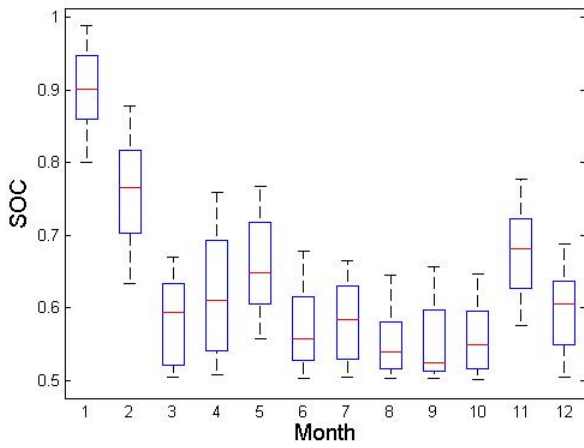


Fig. 6. Monthly SOC of the optimal solution [0 4 0 13 25 1].

VIII. CONCLUSIONS

In this paper, the optimal configuration for an off-grid, renewable energy reverse osmosis desalination system was found using the ant system. Wind, solar and diesel were candidates as well as battery storage. Experiments showed that the ant system converged very well. The optimal configuration with the smallest annualized cost of the renewable energy system was a hybrid wind/photovoltaic/battery system with high yearly average battery state of charge. The annualized cost of the renewable energy system was 15855 USD/year with the corresponding cost of energy as 0.46 USD/ kWh and cost of water as 3.35 USD/m³, which was less than half of the 7.9 USD/m³ currently paid by residents that live in the area. For the optimal solution with a compulsory diesel generator, diesel

mainly was the complement when wind and solar were weak. If this kind of combination was used in real world, frequent equilibrium charging was necessary for the sake of battery lifetime. The 2-kW wind turbine generator was selected among the three types of wind turbine generators.

ACKNOWLEDGMENT

This research was supported by the Science Research Project (No. 16JK1506) of Education Department of Shaanxi Provincial Government, P. R. China.

REFERENCES

- [1] M. A. Abdelkareem, M. El Haj Assad, E. T. Sayed, and B. Soudan, "Recent progress in the use of renewable energy sources to power water desalination plants," *Desalination*, vol. 435, no. September 2017, pp. 97–113, 2018.
- [2] R. Siddaiah and R. P. Saini, "A review on planning, configurations, modeling and optimization techniques of hybrid renewable energy systems for off grid applications," *Renew. Sustain. Energy Rev.*, vol. 58, pp. 376–396, May 2016.
- [3] M. Dorigo, V. Maniezzo, and A. Colorni, "The Ant System: An Autocatalytic Optimizing Process," Technical Report 91-016, 1991.
- [4] C. Blum, "Ant colony optimization : Introduction and recent trends," *Physics of Life Reviews*, vol. 2, pp. 353–373, 2005.
- [5] A. Shekhawat, P. Poddar, and D. Boswal, "Ant colony Optimization Algorithms : Introduction and Beyond," *Artificial Intelligence Seminar 2009*, Indian Institute of Technology, Bombay, 2009.
- [6] M. Haws, "Solar Solar Desalination Using Distillation," *USBR, Res. Dev. Off. Sci. Technol. Program, Final Rep. 2014, Proj. ID 4850*, no. September, 2015.
- [7] V. G. Gude, *Renewable energy powered desalination handbook : application and thermodynamics*. Oxford, United Kingdom: Butterworth-Heinemann, 2018.
- [8] D. Xu, T. Acker, and X. Zhang, "Size optimization of a hybrid PV/wind/diesel/battery power system for reverse osmosis desalination," *J. Water Reuse Desalin.*, vol. 9, no. 4, pp. 405–422, 2019.
- [9] D. Xu and T. Acker, "Optimal sizing of an off-grid, renewable energy reverse osmosis desalination system based on a genetic algorithm," *Desalin. Water Treat.*, vol. 163, pp. 67–82, 2019.
- [10] D. Xu and L. Kang, "Optimal dispatch of unreliable electric grid-connected diesel generator-battery power systems," *Int. J. Emerg. Electr. Power Syst.*, vol. 16, no. 3, 2015.
- [11] J. L. Bernal-Agustín and R. Dufo-López, "Simulation and optimization of stand-alone hybrid renewable energy systems," *Renew. Sustain. Energy Rev.*, vol. 13, no. 8, pp. 2111–2118, Oct. 2009.
- [12] A. Maleki, "Design and optimization of autonomous solar-wind-reverse osmosis desalination systems coupling battery and hydrogen energy storage by an improved bee algorithm," *Desalination*, vol. 435, pp. 221–234, Jun. 2018.
- [13] T. Tezer, R. Yaman, and G. Yaman, "Evaluation of approaches used for optimization of stand-alone hybrid renewable energy systems," *Renew. Sustain. Energy Rev.*, vol. 73, no. January, pp. 840–853, 2017.
- [14] L. E. Hartley, J. A. Martínez-Lozano, M. P. Utrillas, F. Tena, and R. Pedrós, "The optimisation of the angle of inclination of a solar collector to maximise the incident solar radiation," *Renew. Energy*, vol. 17, no. 3, pp. 291–309, Jul. 1999.
- [15] S. Wilcox and W. Marion, "Users Manual for TMY3 Data Sets," Technical Report NREL/TP-581-43156, NREL, 2008.